Target Position Estimation in Radar and Sonar, and Generalized Ambiguity Analysis for Maximum Likelihood Parameter Estimation

RICHARD A. ALTES, SENIOR MEMBER, IEEE

Abstract—Target position estimation in radar and sonar means joint estimation of range and angle in the presence of noise and clutter. The global behavior of a maximum likelihood (ML) position estimator, and the clutter suppression capability of the system, can be written in terms of a range-angle ambiguity function. This function depends upon signal waveform and array configuration, i.e., upon both temporal and spatial characteristics of the system.

Ambiguity and variance bound analysis indicates that system bandwidth can often be traded for array size, and direction-dependent signals can be used to obtain better angle resolution without increasing the size of the array. Wide-band direction-dependent signals (temporal diversity) can be traded for large real or synthetic arrays (spatial diversity). This tradeoff is apparently exploited by some animal echolocation systems.

The above insights are obtained mostly from the properties of the range-angle ambiguity function. In general, an appropriate ambiguity function should be very useful for the design and evaluation of *any* ML parameter estimator. System identification methods and radio navigation systems, for example, can be optimized by minimizing the volume of a multiparameter ambiguity function.

INTRODUCTION

SYSTEM *requirements* for radar, sonar, or diagnostic ultrasound include parameters such as array size, signal bandwidth, and processor complexity (measured by the time–bandwidth product of the signal, data storage capacity, and processing time). System *performance* involves quantities such as estimator variance, resolution, and clutter rejection capability. Performance can be measured in terms of Cramér–Rao (CR) bounds, ambiguity function properties, and signal-to-clutter ratio. If these performance measures can be written in terms of array size, signal bandwidth, and processor complexity (system requirements), then tradeoffs between requirements such as array size and bandwidth can be assessed.

CR bounds [1], [2] provide a local measure of estimator accuracy for particular values of the estimated parameters. In terms of a hypothesis test, CR bounds are useful when the hypothesized parameters are nearly equal to their true values, i.e., when there is good prior information about the parameters that are to be estimated. CR bounds are often obtained by assuming that the data consists of a signal that depends upon the unknown parameters, added to white Gaussian noise (WGN). If the data actually consists of additional, spurious signals (clutter), then the WGN assumption is invalid, and meaningful CR bounds can be obtained only after a more general probability distribution has been worked out.

The ambiguity function [3], [4] illustrates the global properties of a maximum likelihood (ML) estimator. In terms of a hypothesis test, the ambiguity function shows the response of the estimator to *all* possible values of the hypothesized parameters, when the true parameters are specified. Possible confusion between different parameter values can thus be illustrated. Like CR bounds, the ambiguity function is often derived under a WGN assumption, but the effect of spurious echoes can be analyzed in terms of this idealized ambiguity function, and its utility is not restricted to the WGN case [5]–[10]. In view of these properties, it is not surprising that ambiguity analysis often results in the imposition of constraints upon a system design that minimizes a CR bound. For example, the ambiguity function gives the accuracy of prior knowledge that is required for such a system.

We shall consider properties of both CR bounds and the ambiguity function for joint range-angle estimation. Targets that are in the near field of an array, as well as in the far field, will be considered, since the effective size of synthetic aperture arrays is so large that the far-field assumption is often violated. Diagnostic ultrasound arrays for examination of near-surface effects (breast and parotid tumors, carotid artery wall thickness) will sometimes operate in a near-field configuration, and passive sonar systems with widely separated sensors must also be analyzed without far-field assumptions.

The ambiguity function approach to radar/sonar signal design is well established [3], [4], [11], and this paper uses a similar method for combined signal and array (temporal and spatial) design. Ambiguity analysis, however, has apparently been neglected for other parameter estimation problems, and it has been confined to the radar/sonar literature. One purpose of this paper is to illustrate the advantages of multiparameter ambiguity analysis (Kelly and Wishner [12]) in a more general context.

It will be shown that the volume of the ambiguity function provides a measure of the extent to which different parameter estimates can be separated from each other and from a background that may include spurious signals as well as noise. By far the best known ambiguity function is associated with delay and frequency shift measurements, using narrow-band signals [3]. The volume of this ambiguity function depends only upon signal energy, and the resulting volume invariance for

Manuscript received June 28, 1978; revised January 25, 1979. This work was supported by the Biosystems Laboratory of the Naval Ocean Systems Center, Kailua, HI.

The author is with the Orincon Corporation, 3366 N. Torrey Pines Ct., Suite 320, La Jolla, CA 92037.

0018-9219/79/0600-0920$00.75

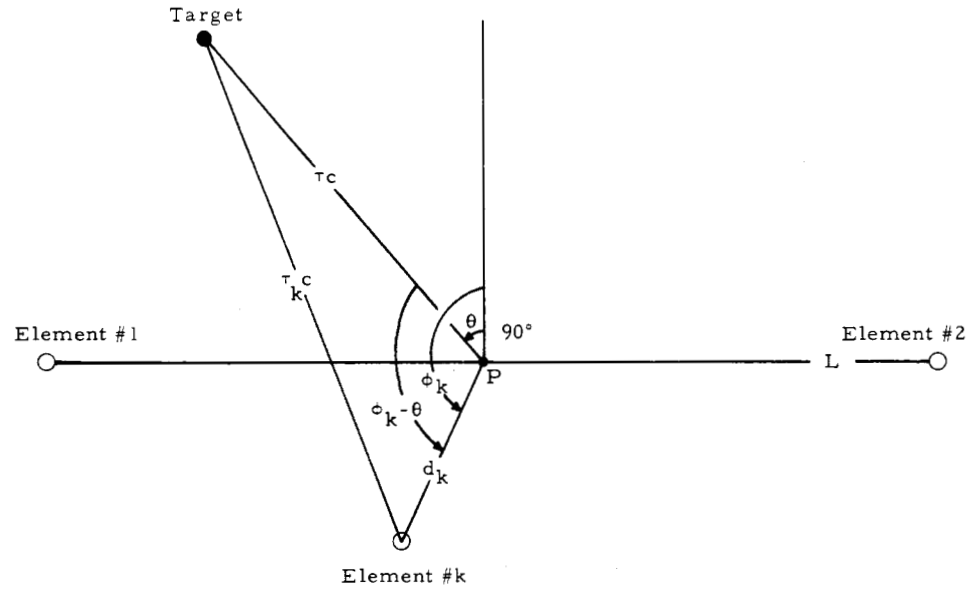

Fig. 1. Definitions of angles and distances for a planar array of receiving elements.

energy normalized signals can be interpreted as a radar uncertainty principle [13]. The volume invariance of the narrow-band range-Doppler ambiguity function is more the exception than the rule, however, [14], [15], and the analysis in this paper demonstrates that *minimization of ambiguity volume can be an important technique for the optimization of a parameter estimator.* Minimization of ambiguity volume should be especially applicable to signal design for system identification, a branch of control theory that has much in common with radar/sonar design.

Animal sonar or echolocation is a biological phenomenon that is especially fascinating to radar/sonar engineers. One of the first proposals for a man-made sonar system was suggested in 1912, after the Titanic disaster, as a simulation of the "sixth sense of the bat" [16], [17]. Photographs of bats in pursuit of insects among foliage [18] seem to indicate a high degree of clutter suppression capability, and the echolocation performance of cetaceans in shallow, reverberation limited environments is also impressive. Animal sonars operate under a significant constraint; their receiving "arrays" consist of only two closely spaced elements. Many echolocating animals, however, have evolved extremely wide-band systems, and the highest frequency is often more than three times larger than the lowest frequency [19]. We know that increasing a signal's bandwidth results in better range resolution [3], [4] and better target discrimination capability [20]-[25], and that large time-bandwidth products can be advantageous for wide-band velocity resolution [26], [27] or for Doppler tolerance [28]-[30]. We also suspect that the use of wide-band signals may be associated with better angle measurements [31], [32], and that *echolocating animals may be able to compensate for limited array size by using larger bandwidths.* The following analysis indicates that this suspicion is well-founded.

For the reader who is interested in radar, sonar, diagnostic ultrasound, and animal echolocation, the paper should provide some useful results and insights. For the reader who is interested in other parameter estimation problems, the specific results are not so important, but the general approach illustrates a useful system design philosophy.

Problem Formulation and General Results

In this section, expressions for CR bounds and the ambiguity function are derived for the position estimation problem. The results will apply to all planar array configurations. No assumptions about array shape or target position will be introduced, except for the simplifying assumption that the target lies in the plane of the receiving array.

Let $E(\omega)$ be the Fourier transform of an echo, measured at the target. The frequency-domain response of the kth array element to the echo is:

$$F_k(\omega) = A_k E(\omega) \exp(-j\omega\tau_k) \tag{1}$$

where

$$A_k \equiv \text{complex gain of the } k\text{th element} \tag{2}$$

$$\tau_k \equiv \text{delay from target to } k\text{th element.} \tag{3}$$

In (1)-(2), it is assumed that the transfer function of the kth array element is constant, i.e., it is independent of direction and frequency. Frequency independence is sometimes associated with a narrow-band assumption, since an element's transfer function is approximately constant over a sufficiently narrow frequency band. The more general case can be investigated by substituting $A_k(\theta, \omega)$ for A_k in the following development, where the direction parameter θ is defined below.

Let L be a straight line segment between the elements of the array that are furthest apart. The range parameter τ is defined as the delay between the target and the center point P of L, i.e., the point that lies midway between the extremities of the array (see Fig. 1). The direction parameter θ is defined to be the angle between the normal to L at P and the line segment between P and the target. Movement of the target counterclockwise around P causes θ to increase, i.e., θ is positive in the counterclockwise direction.

The position of each array element can be defined in the same way as the target position. In Fig. 1, the kth element position is described in terms of the direction parameter ϕ_k and the distance d_k from P, where ϕ_k is the angle between

the normal to L at P and the line segment between P and the array element. From Fig. 1, a general expression for τ_k is

$$\tau_k = [\tau^2 + (d_k/c)^2 - 2\tau(d_k/c)\cos(\phi_k - \theta)]^{1/2} \quad (4)$$

and τ_k depends upon the unknown parameters τ and θ, as well as upon the known parameters d_k and ϕ_k.

The array element responses in the absence of noise can be represented by a column vector $m(\tau, \theta)$ of complex numbers. The first N elements of $m(\tau, \theta)$ are frequency samples of $F_1(\omega)$ in (1). The next N elements are samples of $F_2(\omega)$, etc. For an integration interval T, the N discrete frequency samples are separated by π/T rad/s. For K array elements, m has KN elements.

In representing $F_k(\omega)$ by N discrete frequency samples, it is assumed that the response of the kth element is time limited. Although a time limited signal cannot be band limited, it is assumed that, for any acceptable mean-square error $\epsilon > 0$ between the original time signal and the time signal that is reconstructed from N frequency components, there exists a bounded number N such that the mean-square reconstruction error is less than ϵ.

In Gaussian noise, a data vector r is observed, where the elements of r are the frequency samples of $F_1(\omega), F_2(\omega), \cdots, F_K(\omega)$ when noise has been added to the echo. The conditional probability density function (PDF) of the noisy data is [31]

$$p(r|\tau, \theta) = (\pi^{KN/2}|\bar{C}|)^{-1} \exp -[r - m(\tau, \theta)]^* \bar{Q}[r - m(\tau, \theta)] \quad (5)$$

where $\bar{C} = \bar{Q}^{-1}$ is the noise covariance matrix and the asterisk denotes a conjugate-transpose operation.

In the presence of multiple targets and clutter or reverberation, as well as noise, it is still possible to use a Gaussian PDF as in (5), provided that an appropriate covariance matrix is determined [33]. The PDF in (5) may appear to be unrealistic for sea clutter, since the envelope of a Gaussian clutter process is Rayleigh distributed, while the *measured* PDF of envelope detected sea clutter echoes is often more log-normal than Rayleigh [34], [35]. The empirical log-normal model for the clutter envelope indicates that the underlying PDF of the time domain clutter process decreases more slowly in the "tails" than the Gaussian distribution. The use of a frequency domain representation in (5), however, implies that time domain echoes are effectively passed through a bank of narrow-band filters with impulse responses that are T s long. The sampled responses r of these filters tend to be much more Gaussian than the original time domain distribution [36].

ML estimates of range and angle are the values of τ, θ that maximize $p(r|\tau, \theta)$ in (5) for a given data vector r. The asymptotic variance of these estimates for many observations of the data can be obtained from the matrix CR bound [1], [2]. The CR bound is defined for a *particular value* of τ, θ, and it does not take account of the possibility that two very different parameter pairs τ_1, θ_1 and τ_2, θ_2 may yield nearly equal local maxima of $p(r|\tau, \theta)$. The ambiguity function is a *global* measure of ML estimator performance that reveals the parameter pairs which are most likely to be confused with one another, i.e., which are associated with an ambiguous interpretation of the data. We shall obtain general expressions for both the CR bound and the ambiguity function.

When range τ and angle θ are both unknown, CR bounds for their joint estimates are determined by inverting the Fisher information matrix, $\bar{J}$. The elements of $\bar{J}$ are

$$\begin{aligned} J_{11} &= J_{\tau\tau} = -E[(\partial^2/\partial\tau^2)\ln p(r|\tau, \theta)] \\ J_{12} &= J_{\tau\theta} = -E[(\partial^2/\partial\tau\partial\theta)\ln p(r|\tau, \theta)] \\ J_{21} &= J_{\theta\tau} = -E[(\partial^2/\partial\theta\partial\tau)\ln p(r|\tau, \theta)] \\ J_{22} &= J_{\theta\theta} = -E[(\partial^2/\partial\theta^2)\ln p(r|\tau, \theta)]. \end{aligned} \quad (6)$$

Substituting (5) into (6), we obtain

$$\begin{aligned} J_{\tau\tau} &= 2\partial m^*/\partial\tau\bar{Q}\partial m/\partial\tau \\ J_{\tau\theta} &= 2\ \mathrm{Re}\{\partial m^*/\partial\tau\bar{Q}\partial m/\partial\theta\} \\ J_{\theta\tau} &= 2\ \mathrm{Re}\{\partial m^*/\partial\theta\bar{Q}\partial m/\partial\tau\} \\ J_{\theta\theta} &= 2\partial m^*/\partial\theta\bar{Q}\partial m/\partial\theta \end{aligned}$$

where $m = m(\tau, \theta)$ are the expected responses in (5), i.e., frequency samples of $F_k(\omega)$ in (1), for $k = 1, 2, \cdots, K$. The derivatives in (7) are evaluated at the particular τ and θ values that correspond to the target's true position. The diagonal terms of $\bar{J}^{-1}$ are the CR bounds for the variance of the range and angle estimates $\hat{\tau}$ and $\hat{\theta}$,

$$\begin{aligned} \mathrm{Var}(\hat{\tau} - \tau) &\geq [J_{\tau\tau} - (J_{\tau\theta}J_{\theta\tau}/J_{\theta\theta})]^{-1} \\ \mathrm{Var}(\hat{\theta} - \theta) &\geq [J_{\theta\theta} - (J_{\tau\theta}J_{\theta\tau}/J_{\tau\tau})]^{-1}. \end{aligned} \quad (8)$$

In order to obtain simple mathematical expressions for the above variances, it will be assumed that

$$\bar{Q} = N_0^{-1}I \quad (9)$$

where N_0 is the noise power spectral density and I is the identity matrix. This assumption means that the noise is white and Gaussian, and that the noise at each of the K array elements is statistically independent of the noise at any other element. The CR bounds that are obtained by using (9) are generally not relevant for an environment that includes multiple targets and clutter or reverberation, although it may be possible to approximate a diagonal covariance matrix by using a large integration time T for the computation of the frequency domain samples r [37]. The WGN assumption yields idealized bounds that convey only qualitative information about the relation between system requirements and performance. These qualitative insights, however, can be very important. For example, CR bounds for WGN show that the accuracy of angle estimates are not completely determined by the physical beamwidth of the receiver [31].

Substituting (9) into (7), we have

$$J_{\tau\tau} = 2N_0^{-1}(T/\pi)\int_{-\infty}^{\infty}\omega^2|E(\omega)|^2\,d\omega\sum_{k=1}^{K}|A_k|^2(\partial\tau_k/\partial\tau)^2 \quad (10a)$$

$$J_{\tau\theta} = J_{\theta\tau} = 2N_0^{-1}(T/\pi)\int_{-\infty}^{\infty}\omega^2|E(\omega)|^2\,d\omega\sum_{k=1}^{K}|A_k|^2 \cdot(\partial\tau_k/\partial\tau)(\partial\tau_k/\partial\theta) \quad (10b)$$

$$J_{\theta\theta} = 2N_0^{-1}(T/\pi)\int_{-\infty}^{\infty}\omega^2|E(\omega)|^2\,d\omega\sum_{k=1}^{K}|A_k|^2(\partial\tau_k/\partial\theta)^2. \quad (10c)$$

In (10), τ_k is given by (4) and is shown in Fig. 1. Further

simplifications can be obtained under appropriate assumptions about the relative magnitudes of τ, τ_k, and d_k/c. Some of these simplifications will be discussed in the sequel.

A range-angle ambiguity function is obtained by studying the behavior of the conditional probability density function when we try to determine ML estimates by trial-and-error. This procedure has been utilized by Urkowitz *et al.* [38] to derive an angular ambiguity function $\chi(\theta, \theta_H)$.

The ML estimates τ, θ are the values of the hypothesized range and angle τ_H, θ_H that maximize $p[r|\tau_H, \theta_H]$ or that minimize

$$\epsilon = [r - m(\tau_H, \theta_H)]^* \bar{Q} [r - m(\tau_H, \theta_H)] \tag{11}$$

where

$$r = m(\tau, \theta) + n$$

and where n is a vector of zero-mean complex noise samples.

The mean value of ϵ is the weighted mean-square error between r and $m(\tau_H, \theta_H)$. Since

$$m^*(\tau, \theta) m(\tau, \theta) = \sum_{k=1}^{K} \sum_{n=1}^{N} |F_k(\omega_n)|^2 \tag{12}$$

we see from (1) that $\|m(\tau, \theta)\|$ does not depend upon τ_k, and it is therefore invariant in τ and θ. If $\bar{Q}$ is given by (9), it follows that the mean value of ϵ is minimized when $\chi(\tau, \tau_H, \theta, \theta_H)$ is maximized, where

$$\begin{aligned} \chi(\tau, \tau_H, \theta, \theta_H) &\propto \mathrm{Re}\,\{m^*(\tau, \theta) \bar{Q} m(\tau_H, \theta_H)\} \\ &\equiv \sum_{k=1}^{K} |A_k|^2 (1/2\pi) \\ &\quad \cdot \int_{-\infty}^{\infty} |E(\omega)|^2 \exp\,[j\omega(\tau_k - \tau_{Hk})]\, d\omega \\ &= \sum_{k=1}^{K} |A_k|^2 R(\tau_k - \tau_{Hk}) \end{aligned} \tag{13}$$

where $R(\tau)$ is the autocorrelation function of the echo and, from (4),

$$\tau_{Hk} = [\tau_H^2 + (d_k/c)^2 - 2\tau_H (d_k/c) \cos(\phi_k - \theta_H)]^{1/2}. \tag{14}$$

The trial-and-error ML estimator can be conceptualized as a large number of filters, each matched to a different set of values of the known parameters. The ambiguity function $\chi(\tau, \tau_H, \theta, \theta_H)$ describes the outputs of these filters when a noise-free signal is present at the input to the system. If the ambiguity function is large for more than one set of hypothesized parameter values (τ_H, θ_H), then the introduction of noise can easily lead to erroneous estimates.

The range-angle ambiguity function in (13) was obtained under the WGN assumption (9). Unlike the CR bound for WGN, the ambiguity function in (13) can be applied to the analysis of system performance in the presence of clutter or reverberation and multiple targets [5]–[10]. If a point target is at position τ, θ and a point clutter reflector is at position τ_c, θ_c, the output power of a correlation processor due to the clutter reflector is

$$\text{clutter response}\ (\tau, \theta) \propto |\chi(\tau, \tau_c, \theta, \theta_c)|^2. \tag{15}$$

The expected output power due to a superposition of statistically independent clutter reflectors is

$$\begin{aligned} P_C &= E\,\{\text{clutter response}\ (\tau, \theta)\} \\ &\propto \int_{-\pi}^{\pi} \left[\int_{-\infty}^{\infty} p(\tau_c, \theta_c) |\chi(\tau, \tau_c, \theta, \theta_c)|^2 d\tau_c \right] d\theta_c \end{aligned} \tag{16}$$

where $p(\tau_c, \theta_c)$ is a PDF [5] or scattering function [9] that describes the distribution of clutter in range-angle space.

The correlator response to the target is

$$P_T \propto |\chi(\tau, \tau, \theta, \theta)|^2 \tag{17}$$

and the signal to clutter ratio (SCR) is

$$\mathrm{SCR} = P_T/P_C. \tag{18}$$

For the case when $p(\tau_c, \theta_c)$ is uniform, e.g., when there is no prior knowledge of the clutter distribution, we have

$$\mathrm{SCR}^{-1} = P_C/P_T = \text{normalized volume of}\ |\chi(\tau, \tau_H, \theta, \theta_H)|^2. \tag{19}$$

One of the well-known properties of the narrow-band range-velocity ambiguity function is volume invariance, i.e., the same ambiguity volume is obtained for any energy normalized signal [3]. It would appear that this volume invariance property does not apply to other ambiguity functions, however, e.g., the wide-band range-velocity ambiguity function [14], [15] and the function in (13). In fact, we shall show that range-angle ambiguity volume and SCR depend upon the bandwidth of the radar/sonar system.

An effective beamwidth can also be written in terms of (16). For a target at angle θ, the expected response from clutter at angle θ_c, integrated over range, is the bracketed integral in (16). If this integral is small relative to P_T, then the effective beam pattern has small gain at θ_c when the center of the beam (boresight) is aimed at the target. For uniformly distributed clutter,

$$\text{Effective gain at}\ \theta_c\ \text{with boresight at}\ \theta = P_T^{-1} \int_{-\infty}^{\infty} |\chi(\tau, \tau_c, \theta, \theta_c)|^2\, d\tau_c. \tag{20}$$

We have now obtained expressions for CR bounds and the range-angle ambiguity function, under a WGN assumption. The general target and array description in Fig. 1 has led to comparatively simple notation in (10) and (13), where no assumptions about specific geometries have been introduced (except for a planar array with a coplanar target). These expressions will now be applied to position measurements with a linear array.

Linear Array, Far Field

For a linear array, we have $\phi_k = \pm\pi/2$ for all K array elements. For simplicity of notation, we shall set $\phi_k = -\pi/2$ and we shall allow d_k to be negative as well as positive. In this case, equation (4) becomes

$$\tau_k = \tau[1 + \tau^{-2}(d_k/c)^2 + 2\tau^{-1}(d_k/c) \sin\theta]^{1/2}. \tag{21}$$

If the target is in the far field, we can assume that

$$(d_k/c)^2 \ll \tau^2 \tag{22}$$

and (21) becomes

$$\tau_k \approx \tau + (d_k/c) \sin \theta. \tag{23}$$

Substituting (23) into (10) gives

$$J_{\tau\tau} = \text{SNR}\, D_\omega^2 \tag{24a}$$

$$J_{\theta\theta} = \text{SNR}\, D_\omega^2 D_A^2 \cos^2 \theta \tag{24b}$$

$$J_{\tau\theta} J_{\theta\tau} = (\text{SNR}\, D_\omega^2 M_A \cos \theta)^2 \tag{24c}$$

where

$$\text{SNR} = (T/\pi N_0) \sum_{k=1}^{K} |A_k|^2 \int_{-\infty}^{\infty} |E(\omega)|^2 \, d\omega \tag{25}$$

$$D_\omega^2 = \int_{-\infty}^{\infty} \omega^2 |E(\omega)|^2 \, d\omega \Big/ \int_{-\infty}^{\infty} |E(\omega)|^2 \, d\omega \tag{26}$$

$$D_A^2 = \sum_{k=1}^{K} (d_k/c)^2 |A_k|^2 \Big/ \sum_{k=1}^{K} |A_k|^2 \tag{27}$$

and

$$M_A = \sum_{k=1}^{K} (d_k/c) |A_k|^2 \Big/ \sum_{k=1}^{K} |A_k|^2. \tag{28}$$

Because $J_{\tau\theta} = J_{\theta\tau}$, the product $J_{\tau\theta} J_{\theta\tau}$ in (8) is always nonnegative. For given values of $J_{\tau\tau}$ and $J_{\theta\theta}$, and for $J_{\tau\theta} J_{\theta\tau} \geq 0$, equation (8) indicates that the best performance is obtained when

$$J_{\tau\theta} J_{\theta\tau} = 0. \tag{29}$$

According to (24c) and (28), this condition is obtained in WGN when the array is symmetric about its midpoint, i.e., when

$$d_2 = -d_1, \quad d_4 = -d_3, \cdots$$
$$|A_2|^2 = |A_1|^2, \quad |A_4|^2 = |A_3|^2, \cdots \tag{30}$$

or

$$d_1 = 0, \quad d_3 = -d_2, \quad d_5 = -d_4, \cdots$$
$$|A_3|^2 = |A_2|^2, \quad |A_5|^2 = |A_4|^2, \cdots. \tag{31}$$

When either (30) or (31) is true, equation (8) becomes

$$\text{Var}\,(\hat{\tau} - \tau) \geq [\text{SNR}\, D_\omega^2]^{-1} \tag{32}$$

$$\text{Var}\,(\hat{\theta} - \theta) \geq [\text{SNR}\, D_\omega^2 D_A^2 \cos^2 \theta]^{-1}. \tag{33}$$

Equality in (32) and (33) is asymptotically obtained for a large number of measurements, if a ML estimate is used in WGN (no clutter), and there is accurate prior knowledge of target location.

What, exactly, is meant by "accurate prior knowledge of target location?" How accurate is "accurate?" Does the required accuracy of prior knowledge change when D_ω^2 and/or D_A^2 are increased in (32) and (33)? These questions are often left unanswered in the derivation of parameter estimation methods that are based upon CR bounds, or the problem is sidestepped by *assuming* that the estimates are consistent and unbiased. It will become apparent, however, that ambiguity analysis provides straightforward answers to these questions.

The bounds in (32) and (33) can be minimized by using two elements at opposite ends of the array and a narrow-band signal with the highest allowable frequency. This observation follows easily from the inequalities

$$\int_{-W}^{W} \omega^2 |E(\omega)|^2 \, d\omega \leq W^2 \int_{-W}^{W} |E(\omega)|^2 \, d\omega \tag{34}$$

$$\sum_{k=1}^{K} d_k^2 |A_k|^2 \leq \max_k (d_k^2) \sum_{k=1}^{K} |A_k|^2 \tag{35}$$

which become equalities when the signal energy is concentrated at $\pm W$ and only two array elements with the largest d_k value are used. These solutions, however, have undesirable ambiguity properties. A ML processor should be evaluated not only by CR bounds but also by ambiguity function analysis.

Although significant caveats exist for quantitative analysis of (32) and (33), the bounds are qualitatively significant because they illustrate a basic interdependence between signal (temporal) design and array (spatial) design. This interdependence will become even more apparent when ambiguity functions are considered.

The range-angle ambiguity function for targets in the far field of a linear array is obtained by substituting (23) into (13),

$$\chi(\tau, \tau_H, \theta, \theta_H) = \sum_{k=1}^{K} |A_k|^2 R[\tau - \tau_H + (d_k/c)(\sin \theta - \sin \theta_H)]$$
$$= \chi(\tau - \tau_H, \sin \theta - \sin \theta_H). \tag{36}$$

If θ and θ_H are less than 30°,

$$\chi(\tau, \tau_H, \theta, \theta_H) \approx \sum_{k=1}^{K} |A_k|^2 R[\tau - \tau_H + (d_k/c)(\theta - \theta_H)]$$
$$= \chi(\Delta\tau, \Delta\theta). \tag{37}$$

When the angle hypothesis is correct, we have $\theta_H = \theta$ or $\Delta\theta = 0$, and (36) is proportional to $R(\Delta\tau)$, the echo autocorrelation function. Additional array elements do not affect the structure of $\chi(\Delta\tau, 0)$, and this structure includes many undesirable sidelobes when the signal is narrow band. Fig. 2 shows $\chi(\Delta\tau, \Delta\theta)$ for a narrow-band pulse and with two hydrophones, i.e., for the "optimum" system design that is obtained from CR bounds as in (34) and (35).

For a single target in a clutter-free environment, Fig. 2 indicates that an accurate position estimate can be obtained only if prior knowledge restricts the search area to the central lobe of the ambiguity function. The central lobe becomes more narrow as the signal frequency and the distance between hydrophones increase, so a more accurate estimate implicitly requires better prior knowledge of the estimated parameters. Under clutter-free conditions, one might then expect the two-hydrophone high-frequency system to emerge as the solution of a sequential beam forming procedure [39]. Ironically, such a final result would be a poor starting point for an adaptive beam former, if the system begins without prior knowledge of τ and θ. The optimality of the two-hydrophone configuration depends upon accumulated information (prior probability densities with small variance), and the result is useless without this information.

Far-field range ambiguities depend upon the behavior of $R(\Delta\tau)$, the echo autocorrelation function. $R(\Delta\tau)$ becomes more impulse-like when the bandwidth of the echo is increased,

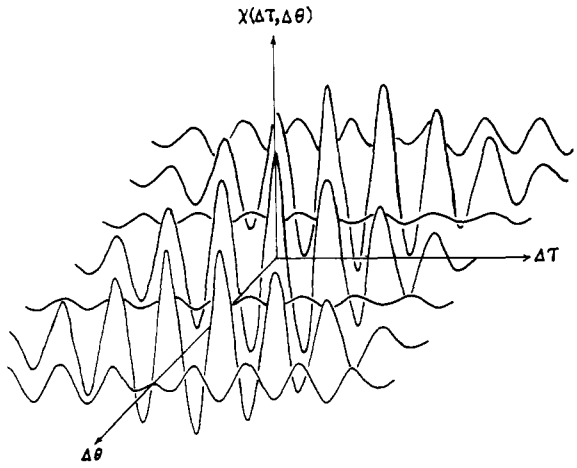

Fig. 2. Two hydrophones, narrow-band pulse. Range-angle ambiguity function for sonar.

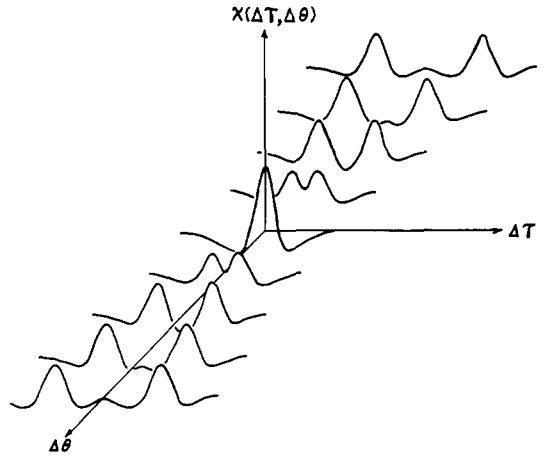

Fig. 3. Wide-band signal, two hydrophones. Range-angle ambiguity function for sonar.

and range ambiguities can be reduced by using a wide-band signal. In the two-hydrophone case, the effect of switching to a wide-band signal is illustrated in Fig. 3.

Fig. 3 illustrates a decomposition of the ambiguity function into a sequence of shifted autocorrelation functions when $\Delta\theta$ becomes large. This effect is predicted by (37). The width of each autocorrelation function is approximately $1/B$ s, where B is the echo bandwidth. If $(d_k/c)\Delta\theta$ is greater than $1/B$ for all k in (37), then a constant $\Delta\theta$ profile of the ambiguity function is a sequence of K nonoverlapping autocorrelation functions, each with amplitude $|A_k|^2$. Decomposition occurs when $|\Delta\theta| > \Delta\theta_0$, where

$$\Delta\theta_0 = (c/B)/\min_k (d_k)$$

$$= \frac{\text{spatial width of echo autocorrelation function}}{\text{minimum distance between hydrophones}}. \tag{38}$$

The ratio in (38) can be small if very large bandwidths are used. In the case of sonar, if $B = 50$ kHz and array elements are 1 m apart, then $\Delta\theta_0 = 0.03$ rad (less than 2°).

For $|\Delta\theta| > \Delta\theta_0$, it is easy to obtain some fundamental properties of the ambiguity function. Since $\chi(\Delta\tau, \Delta\theta)$ for $\Delta\theta$ constant and $|\Delta\theta| > \Delta\theta_0$ is a sum of nonoverlapping autocorrelation functions, we have

$$\max_{\Delta\tau} \chi(\Delta\tau, \Delta\theta)/\chi(0,0)\Big|_{|\Delta\theta| > \Delta\theta_0}$$

$$= \max_k |A_k|^2 R(0) \Big/ \sum_{k=1}^{K} |A_k|^2 R(0)$$

$$\geq 1/K \tag{39}$$

with equality when $|A_k|^2$ is the same for all k values (uniform weighting). The sidelobe level for $|\Delta\theta| > \Delta\theta_0$ can be reduced only by using a larger array. For example, Fig. 4 shows $\chi(\Delta\tau, \Delta\theta)$ for $K = 5$, rather than for $K = 2$, as in Fig. 3.

In terms of SCR, Equation (39) describes the maximum response of the system to a single clutter reflector that is $\Delta\theta$ radians from the target, divided by the response to the target itself. Equation (39) is thus a measure of worst case SCR, where the clutter is restricted to a single point in τ, θ space. For uniformly distributed clutter, SCR for a given value of

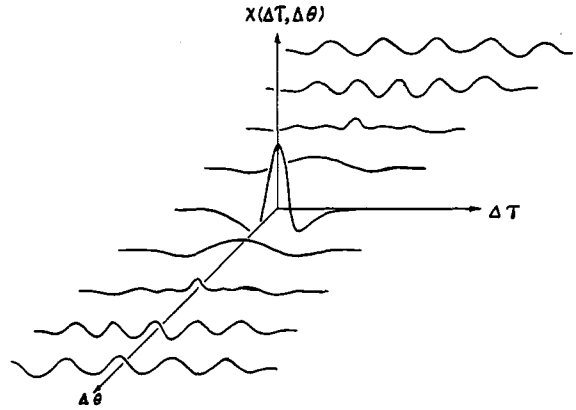

Fig. 4. Wide-band signal, five uniformly spaced hydrophones. Range-angle ambiguity function for sonar.

$\Delta\theta$ is related to the effective beamwidth of the system, as described by (20). Equation (20) gives the receiver response to uniformly distributed clutter that is $\Delta\theta$ radians from the center of the beam. For $|\Delta\theta| > \Delta\theta_0$, Equation (20) becomes

$$\int_{-\infty}^{\infty} |\chi(\Delta\tau, \Delta\theta)|^2 \, d\Delta\tau \Big|_{|\Delta\theta| > \Delta\theta_0} \Big/ |\chi(0,0)|^2$$

$$= \sum_{k=1}^{K} |A_k|^4 \int_{-\infty}^{\infty} |R(\tau)|^2 \, d\tau \Big/ \left| \sum_{k=1}^{K} |A_k|^2 R(0) \right|^2$$

$$= \left\{ \sum_{k=1}^{K} |A_k|^4 \Big/ \left[\sum_{k=1}^{K} |A_k|^2 \right]^2 \right\}$$

$$\cdot \left\{ \int_B |E(\omega)|^4 \, d\omega \Big/ \left[\int_B |E(\omega)|^2 \, d\omega \right]^2 \right\}.$$

By the Cauchy and Schwartz inequalities,

$$\left[\sum_{k=1}^{K} |A_k|^2 \right]^2 \leq K \sum_{k=1}^{K} |A_k|^4$$

$$\left[\int_B |E(\omega)|^2 \, d\omega \right]^2 \leq B \int_B |E(\omega)|^4 \, d\omega \tag{40}$$

and

$$\text{Effective gain } \Delta\theta|_{|\Delta\theta| > \Delta\theta_0} \text{ radians from boresight} \geq 1/KB \tag{41}$$

with equality when $|A_k|^2$ = constant (uniform weighting in space) and when $|E(\omega)|^2$ = constant over B (uniform weighting in frequency). These equality conditions are the converse of the equality conditions for (34) and (35), which minimize CR bounds by using the ultimate in *nonuniform* weighting.

For uniformly distributed clutter, the maximum sidelobe level in (39) is not as relevant as the effective beamwidth measure in (20) and (41). In order to produce a small effective beamwidth for uniformly distributed clutter, the product KB should be large, and system performance depends equally upon bandwidth and array size. For a given array size, clutter suppression performance can be improved by increasing the bandwidth of the system.

A more general measure of SCR is the normalized ambiguity volume in (18) and (19). It is shown in the Appendix that, when $|E(\omega)|^2$ is constant over a bandwidth B,

$$\text{SCR} > B/(2\pi)^2. \tag{42}$$

For uniformly distributed clutter, SCR increases with bandwidth.

An upper bound can be obtained for a two-element system which uses a maximum wavelength λ and a bandwidth B such that

$\lambda \leq$ the distance between receiving elements

$B \geq$ one octave.

These conditions hold for many animal sonar systems, e.g., the bottlenosed dolphin (*Tursiops truncatus*) and the large brown bat (*Eptesicus fuscus*). For these animals,

$$\text{SCR} \leq 2B \tag{43}$$

when clutter is uniformly distributed. Many animal echolocation systems have apparently compensated for their restricted array size by using large bandwidths.

In summary, analysis of the linear array, far-field case has demonstrated that optimization on the basis of CR bounds alone is not a desirable procedure unless the environment is clutter-free and there is good prior knowledge of the estimated parameters. The required accuracy of the prior knowledge can be deduced from an appropriate ambiguity function. *Qualitative* interpretation of CR bounds yields important insight into the fundamental tradeoffs between signal and array parameters. These tradeoffs can be further investigated by computing bounds on SCR, using the range-angle ambiguity function. For uniformly distributed clutter, these bounds depend upon bandwidth alone or upon the product of bandwidth and array size. Array size, independent of bandwidth, becomes important when the clutter consists of a single reflector with particular values of τ and θ.

Linear Array, Near Field

For synthetic aperture systems and for some diagnostic ultrasound and passive sonar applications, targets are often in the near field of the array. The elements of the Fisher information matrix are in this case obtained by substituting (21) into (10). The results are

$$J_{\tau\tau} = \text{SNR}\, D_\omega^2 \sum_{k=1}^{K} \alpha_k^2 |A_k|^2 \Big/ \sum_{k=1}^{K} |A_k|^2 \tag{44a}$$

$$J_{\theta\theta} = \text{SNR}\, D_\omega^2 \cos^2\theta \sum_{k=1}^{K} \beta_k^2 (d_k/c)^2 |A_k|^2 \Big/ \sum_{k=1}^{K} |A_k|^2 \tag{44b}$$

$$J_{\tau\theta} J_{\theta\tau} = \left[\text{SNR}\, D_\omega^2 \cos\theta \sum_{k=1}^{K} \alpha_k \beta_k (d_k/c) |A_k|^2 \Big/ \sum_{k=1}^{K} \cdot |A_k|^2 \right]^2 \tag{44c}$$

where SNR and D_ω^2 were defined in (25) and (26) and

$$\alpha_k = \frac{(d_k/c)\sin\theta + \tau}{\tau_k} = \frac{\text{approximate far-field delay to } k\text{th element}}{\text{actual delay to } k\text{th element}} \tag{45a}$$

$$\beta_k = \tau/\tau_k = \frac{\text{delay to center of array}}{\text{delay to } k\text{th element}}. \tag{45b}$$

The expression for $J_{\tau\tau}$ indicates that the array configuration is important for near-field *range* estimation, a condition that did not exist for far-field measurements. As in the far-field case, $J_{\theta\theta}$ depends upon both temporal and spatial parameters. If the gains A_k are to be adjusted so as to maximize $J_{\tau\tau}$ and $J_{\theta\theta}$, the optimum weights will depend upon target position. This observation suggests that the gains A_k are no longer decoupled from the position hypothesis τ_H, θ_H, *and the gains should change as the environment is scanned.* From (45), the element that is closest to the hypothesized target position should have the largest gain. The expression for $J_{\tau\theta}J_{\theta\tau}$ indicates that the elimination of range-angle error coupling is more difficult to accomplish in the near-field case. This difficulty arises because differences in the near-field delays τ_k depend upon range as well as angle.

The expression for the near-field ambiguity function can be simplified if τ_k in (21) can be written

$$\tau_k \approx \tau\{1 + (1/2)[(d_k/c\tau)^2 + 2(d_k/c\tau)\sin\theta]\}. \tag{46}$$

If the term in square brackets is less than unity, the error in the above approximation is less than 6.4 percent. We are thus assuming that the distance from the target to the center of the array is larger than the array itself. Substituting (46) into (13),

$$\chi(\tau, \tau_H, \theta, \theta_H) = \sum_{k=1}^{K} |A_k|^2 R[s_k\Delta\tau + (d_k/c)(\sin\theta - \sin\theta_H)] \tag{47}$$

where

$$s_k = 1 - [(d_k/c)^2/(2\tau\tau_H)]. \tag{48}$$

The sum in (47) can have an effect that is similar to broadening the bandwidth. When $\theta = \theta_H$, the near-field ambiguity function depends upon a superposition of weighted autocorrelation functions, where each autocorrelation function is scaled by a factor s_k. If the echo autocorrelation function has sidelobes (local maxima at $\Delta\tau \neq 0$), the sum of scaled functions can have a smaller sidelobe level than a sum of unscaled functions, since the maxima for the scaled functions at $\Delta\tau \neq 0$ occur at different locations for different scale factors, s_k. We therefore suspect that the range resolution capabilities

of near-field systems (e.g., synthetic aperture) will often be better than we would predict from the signal autocorrelation function.

When the distance from the target to the array is smaller than the size of the array itself, the best way to obtain a picture of the range-angle ambiguity function is probably to evaluate (13) by means of a computer. A function of τ_H, θ_H can be displayed for any particular values of τ and θ. The effect of sensor positions, gains, and signal bandwidth upon ambiguity volume can then be empirically determined. If ambiguity volume is used as a measure of system performance (SCR), then the optimum signal/array design can be obtained by gradient techniques [40].

Direction-Dependent Signals and Array Elements

The effect of transmitting an angle-dependent signal is to replace $|E(\omega)|^2$ in (13) with $E(\omega, \theta)E^*(\omega, \theta_H)$. If the inverse Fourier transform of $E(\omega, \theta)E^*(\omega, \theta_H)$ has small maximum amplitude for $\theta_H \neq \theta$, the ambiguity function will be rapidly attenuated for $\Delta\theta \neq 0$.

The most common method of achieving direction dependence is through the use of a narrow physical beamwidth. Other methods include the use of a frequency-steered array, a dispersive lens (for sonar), and movement of the array with respect to the environment, so that an angle-dependent Doppler history is obtained from each target. The latter method is employed in synthetic aperture systems [41], [42]. Angle-dependent Doppler shifts could also be used in ultrasonic blood flow measurements, where movement of the target would replace movement of the array.

Direction-dependent array elements can also increase angle resolution [31]. To include the effect of a direction-dependent transfer function, the gain A_k in (2) is replaced by $A_k(\theta)$. More generally, we can take account of the temporal impulse response of the element by using $A_k(\theta, \omega)$. The quantity $|A_k|^2$ in (13) is then replaced by $A_k(\theta, \omega)A_k^*(\theta_H, \omega)$. The effect is again to reduce the level of $\chi(\Delta\tau, \Delta\theta)$ for nonzero $\Delta\theta$.

A direction-dependent receiving element that makes use of multiple reflections, as in the human pinna [43], imposes a direction-dependent convolutional code upon received wide-band waveforms. If the receiver can decode the resulting signal, good angle resolution can be obtained with a very compact physical array. The tradeoff here is between array size and processor complexity.

It is likely that animal echolocation systems exploit direction dependence of transmitted and received signals [31]. A transmitted dolphin echolocation pulse has different structure when it is observed at different angles relative to the animal [19], [32] and the external ears of many bats are capable of imposing a direction-dependent code upon received signals.

Extended Targets and System Identification

The formulation in (11)-(13) can produce a generalized ambiguity function [38] for any ML estimation problem, and it would seem that the ambiguity function should not be restricted to radar/sonar applications. Ambiguity analysis should be especially beneficial for system identification, where CR analysis has already been applied to the design of probing signals [44]-[46]. The shortcomings of signal derivations that are based upon CR bounds alone have already been discussed. It remains to demonstrate the utility of ambiguity analysis for system identification. The advantages of ambiguity analysis should be obvious if we can find a system identification problem that involves radar/sonar measurements. Parameterization of extended targets is ideal for this purpose.

An extended target can sometimes be described as a distribution of point reflectors or highlights in range-angle space. Most diagnostic ultrasound and synthetic aperture imaging systems are based upon such a description. In estimating the position of each highlight, reflections from the other highlights can be regarded as clutter. We have seen that CR bounds, derived under WGN conditions, are not applicable to this situation. An impulse-like ambiguity function, however, will be capable of resolving the target into its separate highlights, or at least of determining the target reflectivity within a small range-angle cell.

An extended target can also be characterized as a distributed parameter system. The impulse response is a function of time (range) for a given angle, and the impulse response changes with angle. The system is to be parameterized by the locations (i.e., the τ, θ values) of large local maxima in the impulse response (i.e., the highlights). Each of these position parameters is to be estimated in the presence of noise and spurious signal components (clutter) that are part of the system's response to the probing signal.

The system identification problem for an extended target is thus equivalent to the estimation of a sequence of τ, θ values in clutter. The ambiguity function is a valuable aid in the design of signals and filters that can perform the required identification. Exclusive use of CR bounds for design of the probing signal for this identification problem can result in an ambiguity function with large volume or large sidelobes, and undesirable interaction between parameter estimates will result. The concept of resolution in radar/sonar performance translates into parameter separability or increased observability in control theory. In a system identification context, the volume of the ambiguity function is a measure of the extent to which each parameter estimate is unaffected by the remaining system parameters.

Conclusion

A range-angle ambiguity function can be used to predict signal-to-interference ratios for high-resolution radar/sonar systems. The expected clutter response will often depend upon the volume under the sidelobes of the ambiguity function, rather than the height of these sidelobes. For a given array size, the sidelobes are made "thinner" by using a wide-band signal, the volume is thus reduced, and signal-to-interference ratio is increased.

Direction-dependent wide-band echoes can result in an impulse-like range-angle ambiguity function. In synthetic aperture systems, the direction dependence is obtained by moving the radar or sonar relative to the environment. Other methods that do not depend upon movement can perhaps be used to increase the rate at which a given area can be mapped. For example, one can use an angle-dependent pulse with large time-bandwidth product, and this signal could be transmitted in all directions simultaneously.

It would seem that the range-angle ambiguity function is a radar/sonar counterpart of the point spread function that is used to define visual acuity. It is therefore a useful concept for sonar systems that are attempting to "see with sound." The tradeoff between bandwidth and array size, which has been obtained from properties of the range-angle ambiguity function, would seem to be important for echolocating animals that use wide-band signals.

CR bounds are helpful indicators of qualitative interdependencies between temporal and spatial parameters. The exclusive use of CR bounds for signal and array synthesis, however, can lead to results which are only optimum in the immediate neighborhood of a particular position, i.e., with accurate prior knowledge of τ and θ. The global behavior of the maximum likelihood estimate is portrayed by the ambiguity function, which provides a more reliable functional for synthesis of signals and array configurations. This observation can be generalized to any parameter estimation problem, and it appears to be especially relevant to the design of probing signals for system identification.

Multiparameter space–time ambiguity analysis can be used to determine the best array locations for passive sonar systems, and the approach is also applicable to signal design and transmitter placement for radio navigation.

In many cases, ambiguity volume depends upon the properties of the estimation device, and a small volume is indicative of paramter separability. Computer minimization of the volume of a multidimensional ambiguity function (especially with a constraint on maximum sidelobe level) should result in an optimum estimating device, e.g., an optimum probing signal for system identification.

Appendix

SCR is defined as the ratio P_T/P_C, where

$$P_T = |\chi(\tau, \tau, \theta, \theta)|^2 \tag{A-1}$$

and

$$P_C \propto \int_{-\infty}^{\infty} d\tau_c \int_{-\pi}^{\pi} d\theta_c \, p(\tau_c, \theta_c) \, |\chi(\tau, \tau_c, \theta, \theta_c)|^2 . \tag{A-2}$$

In (A-2), $p(\tau_c, \theta_c)$ is the clutter probability density function or a normalized version of the clutter scattering function, and

$$\begin{aligned}\chi(\tau, \tau_c, \theta, \theta_c) &= (1/2\pi) \sum_{k=1}^{K} |A_k|^2 \int_{-\infty}^{\infty} |E(\omega)|^2 \\ &\quad \cdot \exp\{j\omega[(d_k/c)(\sin\theta - \sin\theta_c) + \tau - \tau_c]\} d\omega \\ &= \chi(\tau - \tau_c, \sin\theta - \sin\theta_c)\end{aligned} \tag{A-3}$$

for a far-field condition.

For uniformly distributed clutter,

$$\begin{aligned}P_C = (1/2\pi)^2 \sum_{k,n} |A_k|^2 |A_n|^2 \int_{-\pi}^{\pi} d\theta_c \int_{-\infty}^{\infty} d\tau_c \iint_{-\infty}^{\infty} \\ \cdot |E(\omega_1)|^2 |E(\omega_2)|^2 \exp\{j\omega_1[(d_k/c) \\ \cdot (\sin\theta - \sin\theta_c) + \tau - \tau_c]\} \\ \cdot \exp\{-j\omega_2[(d_n/c)(\sin\theta - \sin\theta_c) + \tau - \tau_c]\} d\omega_1 \, d\omega_2 .\end{aligned} \tag{A-4}$$

Performing the τ_c integration, we have

$$(1/2\pi) \int_{-\infty}^{\infty} \exp[-j(\omega_1 - \omega_2)\tau_c] \, d\tau_c = \delta(\omega_2 - \omega_1)$$

and

$$\begin{aligned}P_C = \sum_{k,n} |A_k|^2 |A_n|^2 \int_{-\infty}^{\infty} |E(\omega)|^4 \\ \cdot \exp[j(\omega/c)(d_k - d_n)\sin\theta] \\ \cdot \left\{(1/2\pi) \int_{-\pi}^{\pi} \exp[-j(\omega/c)(d_k - d_n)\sin\theta_c] \, d\theta_c \right\} d\omega .\end{aligned} \tag{A-5}$$

The imaginary part of the θ_c integral is zero, i.e.,

$$-(1/2\pi) \int_{-\pi}^{\pi} \sin[(\omega/c)(d_k - d_n)\sin\theta_c] \, d\theta_c \equiv 0$$

because the integrand is an odd function of θ_c and the limits of integration are symmetric about $\theta_c = 0$. The real part of the θ_c integral is [47]

$$\begin{aligned}(1/\pi) \int_{0}^{\pi} \cos[(\omega/c)(d_k - d_n)\sin\theta_c] \, d\theta_c \\ = J_0[(\omega/c)(d_k - d_n)]\end{aligned}$$

where $J_0(\cdot)$ is a Bessel function of order zero. It follows that

$$\begin{aligned}P_C = \sum_{k,n} |A_k|^2 |A_n|^2 \int_{-\infty}^{\infty} |E(\omega)|^4 J_0[(\omega/c)(d_k - d_n)] \\ \cdot \exp[j(\omega/c)(d_k - d_n)\sin\theta] \, d\omega .\end{aligned} \tag{A-6}$$

The expected clutter response for uniformly distributed clutter is therefore a function of θ, the angle between a line drawn from the center of the array to the target and a line that is normal to the array. An upper bound on P_C can be obtained by noting that

$$\left| J_0[(\omega/c)(d_k - d_n)] \exp[j(\omega/c)(d_k - d_n)\sin\theta] \right| \leq 1$$

and, therefore,

$$P_C \leq \left[\sum_{k=1}^{K} |A_k|^2 \right]^2 \int_{-\infty}^{\infty} |E(\omega)|^4 \, d\omega . \tag{A-7}$$

From (A-1) and (A-3),

$$P_T = \left[(1/2\pi) \sum_{k=1}^{K} |A_k|^2 \int_{-\infty}^{\infty} |E(\omega)|^2 \, d\omega \right]^2 \tag{A-8}$$

and

$$P_T/P_C \geq \left[(1/2\pi) \int_{-\infty}^{\infty} |E(\omega)|^2 \, d\omega \right]^2 \Big/ \int_{-\infty}^{\infty} |E(\omega)|^4 \, d\omega . \tag{A-9}$$

If $|E(\omega)|^2$ is constant over a bandwidth B, then from the equality condition in (40),

$$P_T/P_C \geq B/(2\pi)^2 . \tag{A-10}$$

For uniformly distributed clutter, the lower bound (A-10) on SCR will increase as bandwidth increases.

An upper bound for SCR can be obtained when i) the maximum echo wavelength is less than the minimum distance between hydrophones, and ii) the echo spectral magnitude is smooth and has at least an octave bandwidth. The first condition means that [47]

$$J_0(x) \approx (2/\pi x)^{1/2} \cos(x - \pi/4)$$

where

$$x = (\omega/c)(d_k - d_n).$$

The error in the approximation is less than 3.2 percent for

$$x > 2\pi$$

or

$$\min_{k,n} |d_k - d_n| > \lambda,$$

which is condition (i).

The second condition implies that, for $k \neq n$,

$$\left| \int_{-\infty}^{\infty} |E(\omega)|^4 J_0[(\omega/c)(d_k - d_n)]\, d\omega \right| << \int_{-\infty}^{\infty} |E(\omega)|^4\, d\omega \tag{A-11}$$

because the smooth nonnegative function $|E(\omega)|^4$ is multiplied by a periodic function with at least one full oscillation. Substituting (A-11) into (A-6) and using (A-8), we have

$$P_T/P_C\big|_{\theta=0} \approx \left[\sum_k |A_k|^2\right]^2 \left[\int_{-\infty}^{\infty} |E(\omega)|^2\, d\omega\right]^2 \Big/ \sum_k |A_k|^4 \int_{-\infty}^{\infty} |E(\omega)|^4\, d\omega \tag{A-12}$$

and from (40)

$$P_T/P_C\big|_{\theta=0} \leqslant KB. \tag{A-13}$$

The inequality in (A-11) must be used carefully, since the sum of the left-hand side over a large number of elements may not be small relative to the right-hand side, even though each term of the sum is small. This reservation is inconsequential for studies of animal echolocation, where $K = 2$. The two conditions that lead to (A-13) are satisfied by many wide-band animal echolocation systems. For the Atlantic bottlenose dolphin, *Tursiops truncatus*, echolocation pulses cover a frequency range between about 20 and 150 kHz [19]. The maximum wavelength in water is 7.5 cm, which is shorter than the distance between the ears. The large brown bat, *Eptesicus fuscus*, has a cruising pulse that covers the frequency range between about 25 and 65 kHz [16]. The maximum wavelength in air is 1.3 cm, which is again shorter than the distance between the ears. Although many animals are restricted to two array elements, they can obtain good SCR by using very wide bandwidths.

References

[1] H. Cramèr, *Mathematical Methods of Statistics*. Princeton, NJ: Princeton Univ. Press, 1945.

[2] H. L. Van Trees, *Detection, Estimation, and Modulation Theory, Part I*. New York, Wiley, 1968.

[3] P. M. Woodward, *Probability and Information Theory with Applications to Radar*. Oxford, England: Pergamon, 1964.

[4] C. E. Cook and M. Bernfeld, *Radar Signals*. New York: Academic, 1967.

[5] D. F. DeLong, Jr. and E. M. Hofstetter, "On the design of optimum radar waveforms for clutter rejection," *IEEE Trans. Inform. Theory*, vol. IT-13, pp. 454-463, 1967.

[6] W. D. Rummler, "Clutter suppression by complex weighting of coherent pulse trains," *IEEE Trans. Aerosp. Electron. Syst.*, vol. AES-2, pp. 689-699, 1966.

[7] E. N. Fowle, E. J. Kelly, and J. A. Sheehan, "Radar system performance in a dense-target environment," 1961 IRE Conv. Rec. pt. 4, pp. 136-145, 1961.

[8] C. A. Stutt and L. J. Spafford, "A 'best' mismatched filter response for radar clutter discrimination," *IEEE Trans. Inform. Theory*, vol. IT-14, pp. 280-287, 1968.

[9] H. L. Van Trees, *Detection, Estimation, and Modulation Theory, Part III*. New York: Wiley, 1971.

[10] R. A. Altes, "Suppression of radar clutter and multipath effects for wide-band signals," *IEEE Trans. Inform. Theory*, vol. IT-17, pp. 344-346, 1971.

[11] S. S. Haykin, Ed., *Detection and Estimation, Applications to Radar* (Benchmark papers in Electrical Engineering and Computer Science), vol. 13. Stroudsburg, Dowden, Hutchinson & Ross, 1976.

[12] E. J. Kelly and R. P. Wishner, "Matched filter theory for high-velocity, accelerating targets," *IEEE Trans. Mil. Electron.*, vol. MIL-9, pp. 56-69, 1965.

[13] D. E. Vakman, *Sophisticated Signals and the Uncertainty Principle in Radar*. New York: Springer-Verlag, 1968.

[14] R. J. Purdy and G. R. Cooper, "A note on the volume of generalized ambiguity functions," *IEEE Trans. Inform. Theory*, vol. 14, pp. 153-154, 1968.

[15] R. A. Altes, "Some invariance properties of the wide-band ambiguity function," *J. Acoust. Soc. Amer.*, vol. 53, pp. 1154-1160, 1973.

[16] D. R. Griffin, *Listening in the Dark*. New Haven, CT: Yale Univ. Press, 1958.

[17] H. Maxim, "The sixth sense of the bat. Sir Hiram's contention. The possible prevention of sea collisions," *Scientific Amer.* (Suppl.), pp. 148-150, Sept. 7, 1912.

[18] F. A. Webster, "Interception performance of echolocating bats in the presence of interference," in *Animal Sonar Systems*, vol. 1, R. G. Busnel, Ed. Jouy-en-Josas: Laboratoire de Physiologie Acoustique, 1966.

[19] W. E. Evans, "Echolocation by marine delphinids and one species of fresh-water dolphin," *J. Acoust. Soc. Amer.*, vol. 54, pp. 191-199, 1973.

[20] D. R. Griffin, "Discriminative echolocation by bats," in *Animal Sonar Systems* (see [18]).

[21] R. A. Altes and W. D. Reese, "Doppler tolerant classification of distributed targets—a bionic sonar," *IEEE Trans. Aerosp. Electron. Syst.*, vol. AES-11, pp. 708-723, 1975.

[22] R. A. Altes, "Sonar for generalized target description and its similarity to animal echolocation systems," *J. Acoust. Soc. Amer.*, vol. 59, pp. 97-105, 1976.

[23] D. P. Skinner, R. A. Altes, and J. D. Jones, "Broadband target classification using a bionic sonar," *J. Acoust. Soc. Amer.*, vol. 62, pp. 1239-1246, 1977.

[24] M. E. Bechtel, "Short-pulse target characteristics," in *Atmospheric Effects on Radar Identification and Imaging*, H. E. G. Jeske, Ed. Dordrecht: Reidel, 1976.

[25] R. A. Altes, "Estimation of sonar target transfer functions in the presence of clutter and noise," *J. Acoust. Soc. Amer.*, vol. 61, 1371-1374, 1977.

[26] ——, "Optimum waveforms for sonar velocity discrimination," *Proc. IEEE* (lett.), vol. 59, pp. 1615-1617, 1971.

[27] R. A. Altes and D. P. Skinner, "Sonar velocity resolution with a linear-period-modulated pulse," *J. Acoust. Soc. Amer.*, vol. 61, pp. 1019-1030, 1977.

[28] A. W. Rihaczek, *Principles of High-Resolution Radar*. New York: McGraw-Hill, 1969.

[29] R. A. Altes and E. L. Titlebaum, "Bat signals as optimally Doppler tolerant waveforms," *J. Acoust. Soc. Amer.*, vol. 48, pp. 1014-1020, 1970.

[30] ——, "Graphical derivations of radar, sonar, and communication signals," *IEEE Trans. Aerosp. Electron. Syst.*, vol. AES-11, pp. 38-44, 1975.

[31] R. A. Altes, "Angle estimation and binaural processing in animal echolocation," *J. Acoust. Soc. Amer.*, vol. 63, pp. 155-173, 1978.

[32] M. S. Livshits, "Some properties of the dolphin hydrolocator from the viewpoint of a correlation hypothesis," *Biofizika*, vol. 19, pp. 916-920, 1974 (also JPRS 64329).

[33] L. E. Brennan and I. S. Reed, "Theory of adaptive radar," *IEEE Trans. Aerosp. Electron. Syst.*, vol. AES-9, pp. 237-252, 1973.

[34] M. I. Skolnik, "Sea echo," in *Radar Handbook*, M. I. Skolnik, Ed. New York: McGraw-Hill, 1970, Chap. 26.

[35] D. K. Barton, "Radar measurement accuracy in log-normal clutter," *Eascon'* 71, pp. 246-251, 1971.
[36] A. Papoulis, "Narrow-band systems and Gaussianity," *IEEE Trans. Inform. Theory*, vol. IT-18, pp. 20-27, 1972.
[37] W. S. Hodgkiss and L. W. Nolte, "Covariance between Fourier coefficients representing the time waveforms observed from an array of sensors," *J. Acoust. Soc. Amer.*, vol. 59, pp. 582-590, 1976.
[38] H. Urkowitz, C. A. Hauer, and J. F. Koval, "Generalized resolution in radar systems," *Proc. IRE*, vol. 50, pp. 2093-2105, 1962.
[39] L. W. Nolte and W. S. Hodgkiss, "Directivity or adaptivity?" *Eascon* '75, pp. (35-A)-(35-H), 1975.
[40] D. G. Luenberger, *Optimization by Vector Space Methods*. New York: Wiley, 1969, Chap. 10.
[41] W. M. Brown and L. J. Porcello, "An introduction to synthetic-aperture radar," *IEEE Spectrum*, pp. 52-62, Sept. 1979.
[42] L. J. Cutrona, "Comparison of sonar system performance achievable using synthetic-aperture techniques with the performance achievable by more conventional means," *J. Acoust. Soc. Amer.*, vol. 58, pp. 336-348, 1975.
[43] D. W. Batteau, "Role of the pinna in localization: Theoretical and physiological consequences," in *Hearing Mechanisms in Vertebrates*, De Reuck and Knight, Eds. London, England: Churchill, 1968.
[44] R. K. Mehra, "Optimal input signals for parameter estimation in dynamic systems-survey and new results," *IEEE Trans. Automat. Contr.*, vol. AC-19, pp. 753-768, 1974.
[45] G. D. Swanson, "Biological signal conditioning for system identification," *Proc. IEEE*, vol. 65; pp. 735-740, 1977.
[46] M. Aoki and R. M. Staley, "On input signal synthesis in parameter identification," *Automatica*, vol. 6, pp. 431-440, 1970.
[47] M. Abramowitz and I. A. Stegun, Eds., *Handbook of Mathematical Functions* (NBS Applied Math. Series 55). Washington, DC: U.S. Govt. Printing Office, 1964.

The Processing of Hexagonally Sampled Two-Dimensional Signals

RUSSELL M. MERSEREAU, SENIOR MEMBER, IEEE

Invited Paper

Abstract—Two-dimensional signals are normally processed as rectangularly sampled arrays; i.e., they are periodically sampled in each of two orthogonal independent variables. Another form of periodic sampling, hexagonal sampling, offers substantial savings in machine storage and arithmetic computations for many signal processing operations. In this paper, methods for the processing of two-dimensional signals which have been sampled as two-dimensional hexagonal arrays are presented. Included are methods for signal representation, linear system implementation, frequency response calculation, DFT calculation, filter design, and filter implementation. These algorithms bear strong resemblances to the corresponding results for rectangular arrays; however, there are also many important differences. Some comparisons between the two methods for representing planar data will also be presented.

I. Introduction

BAND-LIMITED two-dimensional signals can be sampled and processed as arrays of numbers. This is both well known and fundamental. Less well appreciated is the knowledge that there are many strategies by which this sampling can be performed, each of which represents a different generalization of one-dimensional periodic sampling. These alternate sampling strategies differ in their assumptions about how the continuous waveform is band limited, in the number of samples that must be taken, and in the efficiency of the resulting signal processing algorithms. Importantly, rectangular sampling, the most common approach, is generally not the most efficient.

With rectangular sampling a band-limited function of two independent variables is sampled at evenly spaced values of each of those variables. It has been the method of choice for virtually all signal processing applications for a variety of reasons: algorithms for processing signals which have been rectangularly sampled can be straightforwardly generalized from the one-dimensional case; the resulting expressions can be readily understood and implemented in software; and hardware to perform the sampling (scanning) is straightforward to build. In fact, we have become so comfortable with rectangularly sampled arrays that the alternatives are rarely considered. Petersen and Middleton [1], however, showed in 1962 that rectangular sampling is a special case of a more general sampling strategy by which a band-limited waveform is sampled on a skewed (i.e., nonorthogonal) sampling raster. Hexagonal sampling is another special case of this general strategy. It is the optimal sampling scheme for signals which are band limited over a circular region of the Fourier plane, in the sense that exact reconstruction of the

Manuscript received October 16, 1978; revised January 29, 1979. This work was supported by the U.S. Army Research Office under Grant DAAG29-76-G-0226 and under Contract DAAG29-78-C-0005.

The author is with the School of Engineering, Georgia Institute of Technology, Atlanta, GA 30332.

0018-9219/79/0600-0930$00.75